Clays and Clay Minerals, Vol. 62, No. 4, 267–285, 2014.

MINERALOGY, GEOCHEMISTRY, AND GENESIS OF MUDSTONES IN THE UPPER MIOCENE MUSTAFAPAŞA MEMBER OF THE ÜRGÜP FORMATION IN THE CAPPADOCIA REGION, CENTRAL ANATOLIA, TURKEY

TACİT KÜLAH[1], SELAHATTİN KADİR[1,*], ALİ GÜREL[2], MUHSİN EREN[3], AND NERGİS ÖNALGİL[1]

[1] Eskişehir Osmangazi University, Department of Geological Engineering, TR-26480 Eskişehir, Turkey
[2] Niğde University, Department of Geological Engineering, TR-51200 Niğde, Turkey
[3] Mersin University, Department of Geological Engineering, TR-33343 Mersin, Turkey

Abstract—The Upper Miocene Mustafapaşa member of the Ürgüp Formation in the Cappadocia region consists predominantly of mudstones, sandstone, and conglomerate lenses with ignimbrite and basalt intercalations. The mudstones are an important source of raw materials for the ceramics industry in Turkey. A detailed mineralogical, geochemical, and genesis study of these materials has not been performed previously and the present study aims to fill that gap. The characteristics of mudstones of the Mustafapaşa member were examined using X-ray diffraction, scanning and transmission electron microscopy, energy dispersive spectroscopy, and chemical analyses. Weathering products of ophiolitic and pyroclastic rocks were transported into the tectonically subsided zone where they accumulated as fluvial and lacustrine deposits. Weathering in the mudstones is evidenced by smectite flakes associated with relict pyroxene, rod-like amphibole, feldspar, and volcanic glass. The chemical composition of mudstones and their distribution suggest that the depositional basin was supplied with ophiolitic material in the south and ignimbrite material in the north. This interpretation is based on an increase in the quantity of feldspar and opal-A and a decrease in the Fe_2O_3+MgO/Al_2O_3+SiO_2 ratio from south to north in the study area. The northward increases in Light Rare Earth Elements/Heavy Rare Earth Elements, La/Yb, Zr/Ni and Zr/Co ratios and Nb, Ba, Rb, Sr, and Eu in the mudstones of the Mustafapaşa member with positive Eu anomalies suggest that the Fe, Mg, Al, and Si required to form smectite were supplied mainly through the decomposition of amphiboles, pyroxenes, feldspars, and volcanic glass during weathering processes. After the deposition of mudstones, relative increases in evaporation-controlled Ca, K, and Al in pore water favored the partial dissolution of Ca-bearing minerals and smectite flakes and *in situ* precipitation of calcite and traces of illite fibers under alkaline micro-environmental conditions during early diagenesis.

Key Words—Cappadocia, Ignimbrite, Mudstone, Ophiolite, Smectite, Turkey, Weathering.

INTRODUCTION

The study area occupies ~400 km^2 in the Cappadocia region in central Anatolia (Turkey), which contains widespread argillaceous sediments of the Upper Miocene Mustafapaşa member of the Ürgüp Formation. In recent decades, extensive attention to the sedimentology, mineralogy, and geochemistry of mudstones has led to significant advances relating to cement, ceramics, and shale gas (*e.g.* Casciello *et al.*, 2011; Chermak and Schreiber, 2014; Osborn *et al.*, 2014; Taylor and Macquaker, 2014). Most published studies of the area are related to volcanism, mineralogy-petrography, and tectonics (Pasquarè, 1968; Pasquarè *et al.*, 1988; Batum, 1975, 1978; Innocenti *et al*., 1975; Besang *et al.*, 1977; Ercan *et al.*, 1987, 1989; Göncüoğlu and Toprak, 1992; Le Pennec *et al*., 1994; Druitt *et al*., 1995; Schumacher and Mues-Schumacher, 1996; Gevrek, 1997; Türkecan *et al*., 2003; Viereck-Götte and Gürel, 2003; Le Pennec *et al*., 2005). Less work has been done on the mineralogy and distribution of Pliocene clay-rich sediments in vertical stacked paleosol levels among ignimbrites (Gürel and Kadir, 2006). The geology and mineralogy of the Upper Miocene and paleosol and carbonate levels and their vertical distributions are used as clues to determine the paleoclimatic conditions of Anatolia and the Mediterranean region (Gürel and Kadir, 2008; Kadir *et al*., 2013; Göz *et al*., 2014). To date, no detailed study has been carried out of the mineralogy, geochemistry, and genesis of these smectitic materials in the Upper Miocene Mustafapaşa member of the Cappadocia Basin. The implications of ophiolitic and volcanic sources for deposits which contain several hundred million tons of clay reserves of potential raw material (for use in cement, ceramics, and elsewhere) also need to be understood. The present study focuses on the mineralogy and geochemistry of the mudstone of the Mustafapaşa member and associated sediments and interprets the genetic relationship between argillaceous sediments and ophiolitic rocks and the Yeşilhisar conglomerate, including ophiolitic components and ignimbrites.

* E-mail address of corresponding author:
skadir_esogu@yahoo.com
DOI: 10.1346/CCMN.2014.0620403

MATERIALS AND METHODS

In the field, representative stratigraphic sections were measured to study the lateral and vertical variations in the Mesozoic ophiolitic rocks, the Oligo-Miocene Yeşilhisar conglomerate, the mudstone of the Upper Miocene Mustafapaşa member, and the ignimbrite. One hundred and seventeen (117) characteristic samples were collected from these units (Figure 3). Fresh and partially altered samples were examined under a polarizing microscope (Leitz Laborlux 11 Pol).

The mineralogical characteristics of the samples were determined by powder X-ray diffraction (XRD) at the Turkish Petroleum Corporation (TPAO, Ankara, Turkey) using a Rigaku Geigerflex instrument. The XRD analyses were performed using CuKα radiation with a scanning speed of 1º2θ min^{-1}. Randomly oriented mounts of powdered whole-rock samples were scanned to determine the mineralogy of each bulk sample. Samples for clay analyses (<2 μm) were prepared by separating the clay fraction using sedimentation and centrifuging the suspension after an overnight dispersion in distilled water. The clay particles were dispersed using ultrasonic vibration for ~15 min. Oriented specimens of the <2 μm fractions were prepared from each sample using the following procedure: drying with air, solvating with ethylene glycol at 60ºC for 2 h, and thermal treatment at 550ºC for 2 h. Semi-quantitative abundances of rock-forming minerals were obtained using Brindley's (1980) external standard method. The relative abundances of clay-mineral fractions were determined using their basal reflections and the mineral intensity factors of Moore and Reynolds (1989).

Scanning electron microscopy (SEM) studies were performed at Eskişehir Osmangazi University (Turkey) using a JEOL JSM 84A instrument equipped with an EDX detector. Representative clay-dominated bulk samples were prepared for SEM analyses by adhering the fresh, broken surface of each sample to an aluminum sample holder with double-sided tape and coating thinly (350 Å) with gold using a Giko ion coater. Transmission electron microscopy (TEM) studies were performed at Anadolu University (Eskişehir, Turkey) using a JEOL JEM-21007 instrument. The clay particles for TEM analyses were dispersed using an ultrasonic ethanol bath for ~30 min. One drop of each clay suspension was placed on carbon-coated copper grids and dried at room temperature.

Chemical analyses of 29 ophiolite and related Yeşilhisar conglomerate, mudstone and ignimbrite whole-rock samples were performed at Acme Analytical Laboratories Ltd. (Vancouver, Canada) using inductively coupled plasma-atomic emission spectroscopy (ICP-AES) for major and trace elements and inductively coupled plasma-mass spectrometry (ICP-MS) for rare-earth elements (*REE*). The detection limits for the analyses were between 0.01 and 0.1 wt.% for major elements, 0.1 and 5 ppm for trace elements, and 0.01 to 0.5 ppm for *REE*.

Smectite structural formulae were determined for the chemical analyses of <2 μm clay fractions of smectite (confirmed by XRD). The samples were prepared by separating the clay fraction using sedimentation followed by centrifugation of the suspension after an overnight dispersion in distilled water. They were then analyzed using ICP-AES at Acme Analytical Laboratories Ltd. (Vancouver, Canada). The structural formulae of smectite were calculated from chemical analyses based on the 22 oxygen atom content of the unit cell (Moore and Reynolds, 1989).

GEOLOGICAL SETTING AND DEPOSITIONAL ENVIRONMENT

Geological setting

The basement rocks of the Cappadocia region comprise Mesozoic ophiolitic rocks consisting of serpentinized peridotites and pyroxenites, isotropic gabbros, diabasic dikes, and extrusive rocks (Dilek and Whitney, 1997). The ophiolitic rocks were thrust onto Paleozoic metamorphic rocks, including gneiss and marble. The region was later subjected to an extensional tectonic regime from the Middle Miocene until the Early Pliocene, which caused the occurrence of a depressional basin in central Anatolia (Toprak, 1998). This subsided basin is filled with fluvial and lacustrine sediments and pyroclastic rocks.

The Oligo-Miocene Yeşilhisar conglomerate typically comprises ophiolitic and metamorphic rock fragments and Neogene sediments. The Yeşilhisar conglomerate overlies discordantly the basement rocks (Figures 1 and 2) and is overlain unconformably by Neogene sediments of the Ürgüp Formation (Pasquarè, 1968). The Upper Miocene Mustafapaşa member is the oldest sedimentary unit in the Ürgüp Formation, which consists of massive and layered mudstones and conglomerates and sandstones of fluvial and lacustrine origin. The Mustafapaşa member overlies ophiolitic basement rocks near the Akköy and Keşlik villages and the Yeşilhisar conglomerate to the south of Yeşilhisar. The sediments of the Mustafapaşa member near the Damsa Valley south of Ürgüp are intercalated locally with the Kavak ignimbrite, a welded, thickly bedded, dark gray Sarımadentepe ignimbrite, and Damsa Valley basaltic lava. The Mustafapaşa member is overlain conformably by Late Miocene to Pliocene volcaniclastic and sedimentary units, which are overlain discordantly by Quaternary ashfall deposits, white travertine, and alluvium (Figure 2, Viereck-Götte *et al.*, 2010).

Description of the lithology

In the study area, the following lithologies have been distinguished in the Oligo-Miocene and Upper Miocene sediments (Figures 3, 4).

https://doi.org/10.1346/CCMN.2014.0620403 Published online by Cambridge University Press

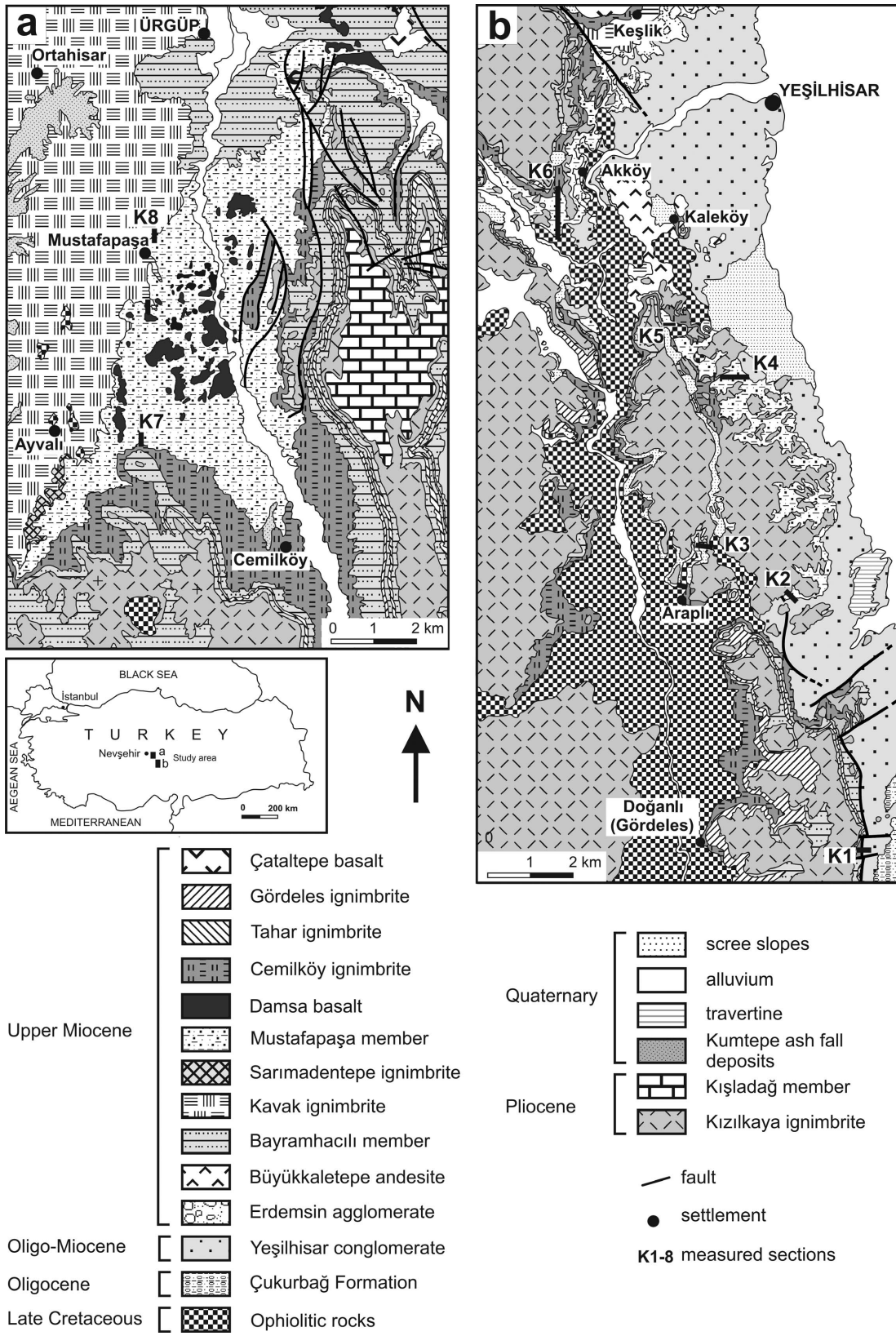

Figure 1. Simplified geological map of the Cappadocia region (after Pasquarè, 1968).

https://doi.org/10.1346/CCMN.2014.0620403 Published online by Cambridge University Press

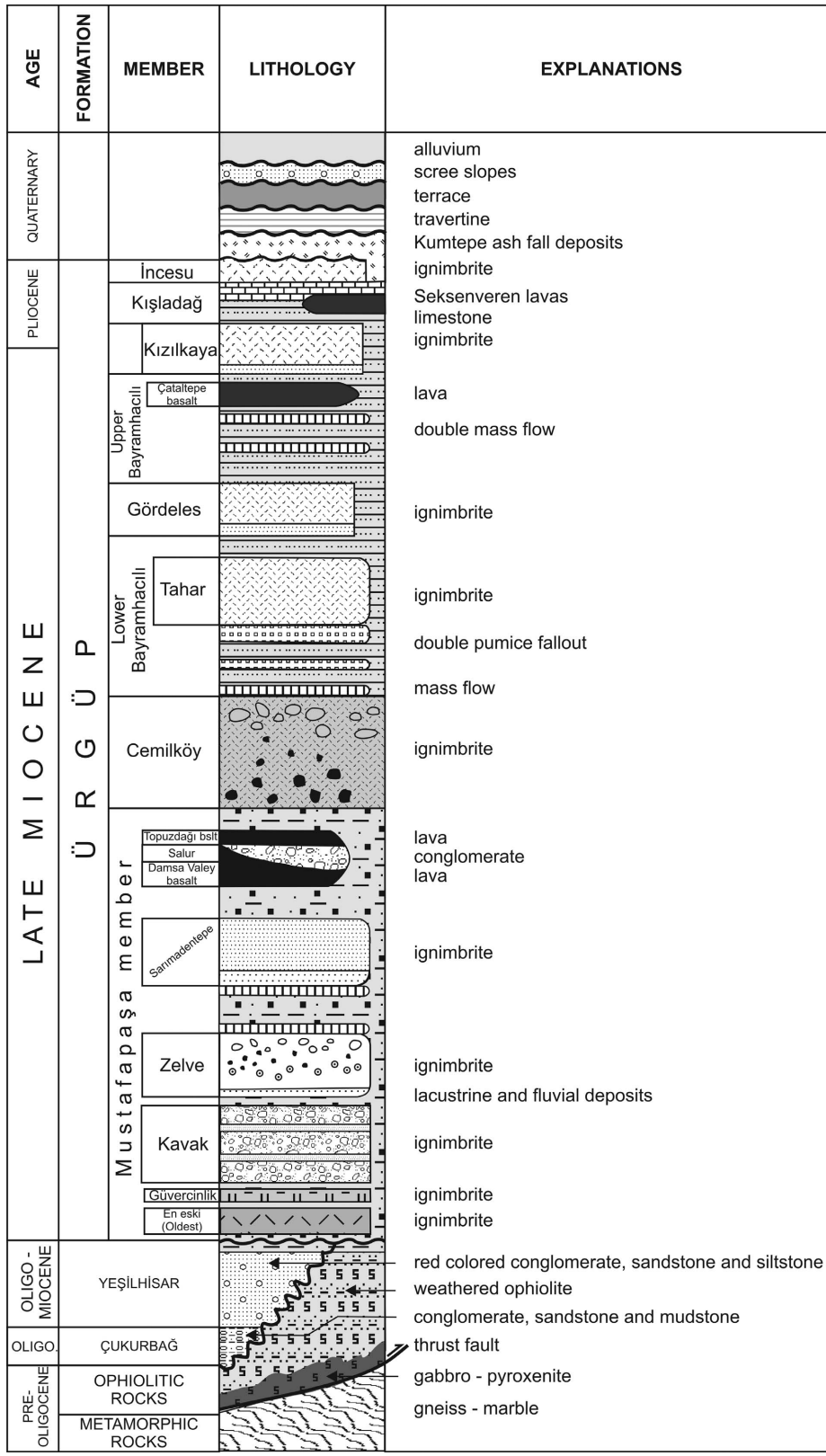

Figure 2. Generalized stratigraphic column of the study area (after Viereck-Götte *et al.*, 2010).

https://doi.org/10.1346/CCMN.2014.0620403 Published online by Cambridge University Press

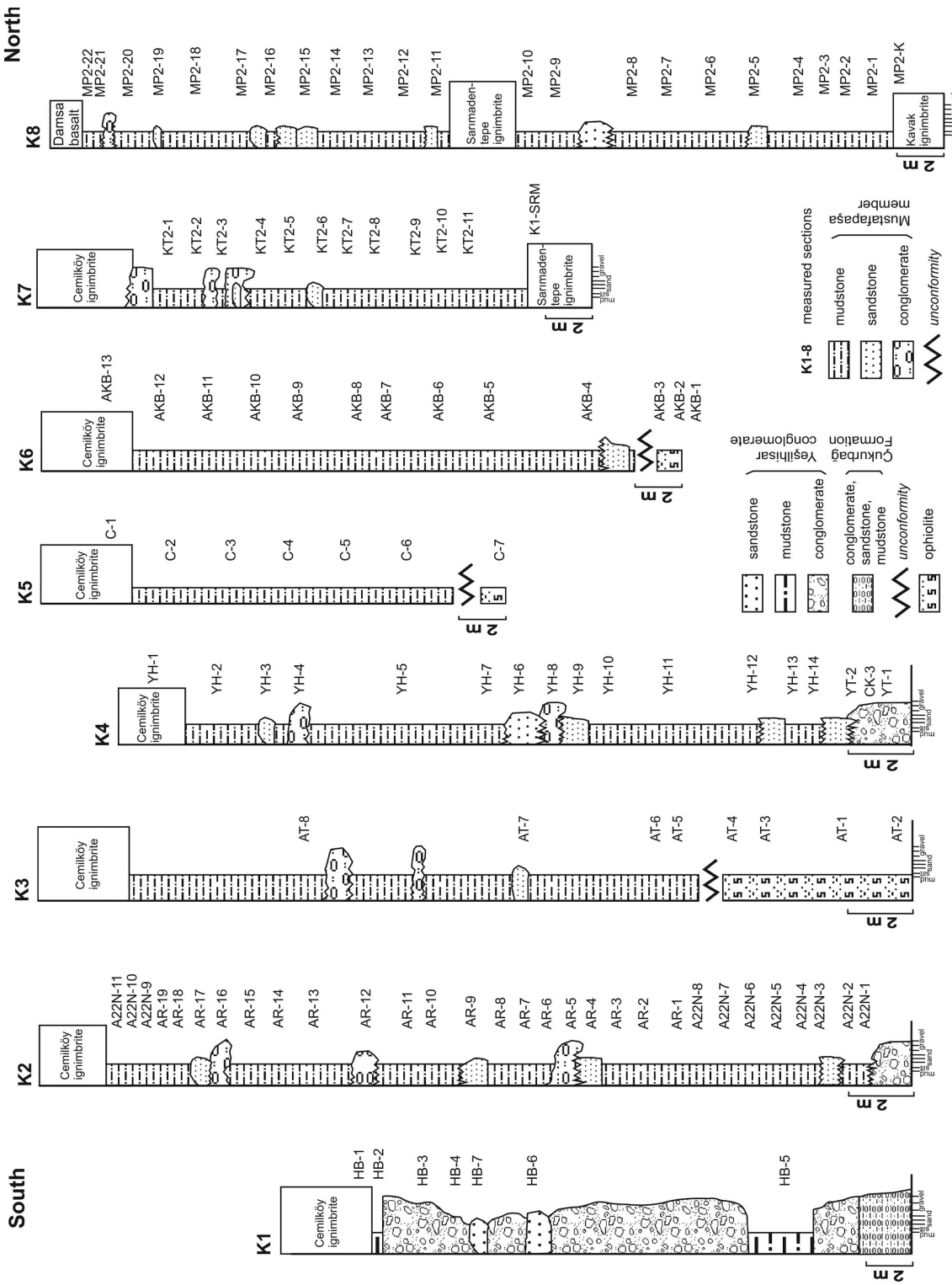

Figure 3. Distribution of the principal lithologies in the study area (see Figure 1 for section locations and Table 1 for the mineralogical compositions of the selected samples).

https://doi.org/10.1346/CCMN.2014.0620403 Published online by Cambridge University Press

Conglomerate. This facies appears in two stratigraphic levels characterized by thick-bedded fluvial sediments of the Yeşilhisar conglomerate (Figure 4a,b) and channel filling in the mudstone of the Mustafapaşa member. The Yeşilhisar conglomerate consists almost entirely of conglomerates, including ophiolitic and metamorphic rock fragments. The pebbles are well rounded and their size varies from a few cm to 20–30 cm. To the north, metamorphic components predominate in these conglomerates. The matrix of the conglomerate consists of red, sandy, silty, and argillaceous material. This lithology appears in an area ~40 km long and 10 km wide. The channel-filling conglomerates in the mudstone of the Mustafapaşa member are characterized by massive, gray, unsorted, and sub-rounded conglomerates. The conglomerates are mainly matrix-supported. The average size of the clasts is ~10 cm. The thickness of the conglomerate varies from 20 to 50 cm. This conglomerate channel has a lenticular character with a cross-section ~2 m wide.

Sandstone. This facies consists of greenish-gray, medium- to fine-grained, medium-bedded sandstones with plant rootlets. The facies is ~50 cm thick and several km long.

Mudstone. This massive and layered mudstone facies appears in two stratigraphic levels characterized by different colors (Figure 4c,d). The lower level is generally greenish-gray, but the upper level is brownish-red. The facies includes plant rootlets and desiccation cracks. The mudstone is ~70 m thick, 10 km wide, and 60 km long.

Description of stratigraphic sections

Eight stratigraphic sections were analyzed from south to north in the study area, and the results are described below (Figure 3, K1–K8).

Hacibekirli section (K1). The Yeşilhisar conglomerate unconformably overlies the Çukurbağ Formation, which is overlain by the Cemilköy ignimbrite (Gürel *et al.*,

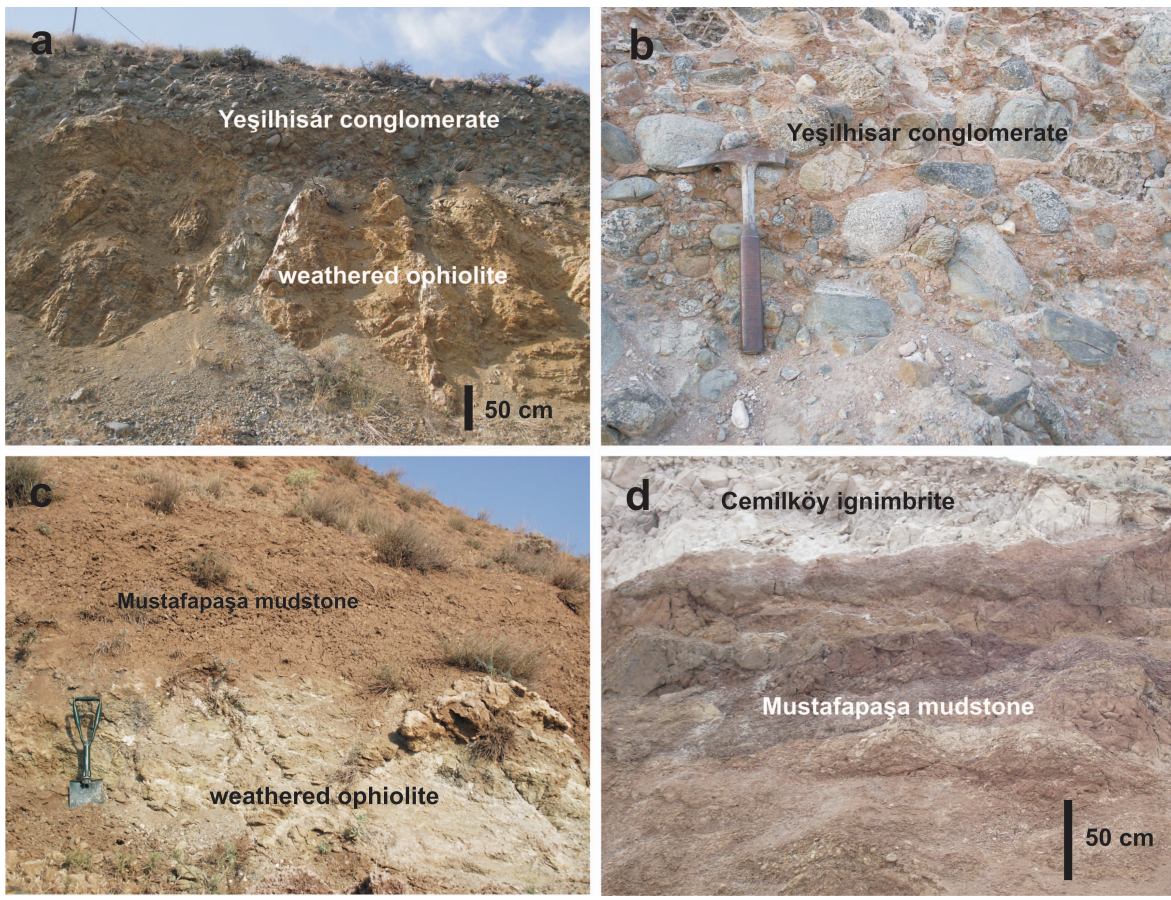

Figure 4. Field view of: (a) the weathered ophiolitic unit and the overlying Yeşilhisar conglomerate; (b) close-up view of ophiolite-sourced pebbles in a matrix of mudstone in the Yeşilhisar conglomerate; (c) mudstone of the Mustafapaşa member on the weathered ophiolitic units; and (d) close-up view of the Mustafapaşa mudstone with intercalated sandstone lenses and overlain by the Cemilköy ignimbrite.

https://doi.org/10.1346/CCMN.2014.0620403 Published online by Cambridge University Press

2007; Figure 3). The section consists predominantly of ophiolitic conglomerate and sandstone and mudstone horizons. These units are overlain by the Cemilköy ignimbrite.

Araplı Pass section (K2). This section begins with the Yeşilhisar conglomerate, which overlies unconformably ophiolitic rocks and is overlain unconformably by mudstones, sandstones, and conglomerates of the Mustafapaşa member (Figure 4a). The Yeşilhisar conglomerate consists of pebbles and cobbles derived predominantly from ophiolitic basement rocks, such as gabbro, pyroxenite, and serpentinite and minor amounts of marble and gneiss (Figure 4b). This section is covered by the Cemilköy ignimbrite.

Araplı section (K3). The ophiolitic basement rocks show signs of weathering. This unit is overlain unconformably by the Mustafapaşa member deposits which consist of mudstones intercalated with sandstones and conglomerate lenses (Figure 4c). The Cemilköy ignimbrite occurs in the uppermost part of this section (Figure 4d).

Yeşilhisar section (K4). This section begins with an ophiolitic unit that is overlain unconformably by the Yeşilhisar conglomerate, which is overlain unconformably by the sediments of the Mustafapaşa member. This section is covered by the Cemilköy ignimbrite.

Çevliktaş Tepe section and Akköy section (K5, K6). The ophiolitic basement rocks are overlain unconformably, mainly by mudstone deposits of the Mustafapaşa member, which is overlain by the Cemilköy ignimbrite.

Kolkollu Tepe section (K7). This section begins with the Sarımadentepe ignimbrite, which is overlain by Mustafapaşa member sediments and topped by the Cemilköy ignimbrite. The thicknesses and frequency of occurrence of conglomerate lenses in the Mustafapaşa member are less than in the southern area. A reddish color is predominant in the Mustafapaşa-member sediments compared with those of previously described sections.

Mustafapaşa section (K9). This section begins with the Kavak ignimbrite, which is overlain by Mustafapaşa-member sediments composed of mudstones intercalated with sandstone and conglomerate lenses and the Sarımadentepe ignimbrite. This section is topped by the Damsa Valley basalt.

PALEOGEOGRAPHY

Tectonic activity during the Oligocene caused the uplift and emergence of the region, after which ophiolitic basement rocks and ignimbrites were subjected to moderate to intensive weathering. Weathering products were eroded, transported, and deposited in the subsided basin. The Yeşilhisar conglomerate, consisting mainly of ophiolitic components, was deposited close to the source area in these valleys. Thin lacustrine sediments were deposited in areas to the north. Polygenetic volcanoes were active in the Late Miocene and their pyroclastic products, such as the Kavak and Sarımadentepe ignimbrites, were intercalated with mudstones in the northern part of the study area (Pasquarè, 1988; Toprak, 1998; Le Pennec *et al.*, 2005). During the arid climatic conditions at the beginning of the Late Miocene, the lacustrine areas were subjected to flash flooding, which caused the deposition of mud and the development of mud flats. Argillaceous sediments then formed in the region (Kadir *et al.*, 2013). According to the profiles examined, the main lithofacies consist of massive and layered mudstones, which occur in three sections: the very shallow part of the lake (southern lake margin, Figure 3, K1, K2), the central part of study area around Akköy (Figure 3, K3, K4, P5, K6), and a shallow-lake environment (north, Figure 3, K7, K8). In the depressional basin, the main paleo-flow direction was generally determined to have been from south to north, based on field observations such as pebble orientation, planar and trough cross-beddings in sandstones, and the mineralogical compositions of detrital sediments.

RESULTS

Mineralogical and petrographical determinations

Ophiolitic rocks are generally composed of serpentinized amphibole, pyroxene, and accessory olivine (Dilek and Furnes, 2014). The Yeşilhisar conglomerate includes components derived mainly from basement rocks. These components consist of serpentinized and Fe (oxyhydr)-oxide-bearing amphibole, pyroxene, and olivine minerals with partial to extensive alteration (Nahon *et al.*, 1982; Delvigne, 1998). Volcanic rocks include plagioclase and amphibole phenocrysts in a volcanic glass groundmass. Feldspars and amphiboles are altered, and the volcanic glass is devitrified.

The XRD results of the bulk samples from the measured profiles are given in Table 1. Smectite is dominant in all of the samples from the sections of the Mustafapaşa member and is accompanied by feldspars, quartz, amphiboles, pyroxenes, calcite, local olivine, and traces of illite/mica, kaolinite, chlorite, and serpentine. The quantities of feldspar and opal-A increase from south to north in the study area.

Smectite is identified by a sharp basal reflection at 14.48–14.91 Å, which shifts to 17.51–17.65 Å following ethylene-glycol treatment and collapses to 10.08–10.13 Å after heating at 550ºC for 2 h (Figure 5). The d_{060} value of smectite is 1.50 Å, suggesting a dioctahedral character (Moore and Reynolds, 1989). Illite/mica is identified by reflections

https://doi.org/10.1346/CCMN.2014.0620403 Published online by Cambridge University Press

Table 1. Mineralogical composition and abundance of samples in the measured sections. Sections and their samples are ordered from north to south.

Sample	Rock type	smc	ilt/mc	kln	chl	srp	am	px	ol	fds	qz	op	cal
North													
K8													
MP2-22	Mudstone	++++	acc							acc	+	acc	acc
MP2-21	Mudstone	+++	acc		acc	acc				+	+	+	
MP2-20	Mudstone	+++								+	+	+	
MP2-16	Mudstone	+++		acc						+	+	acc	
MP2-14	Mudstone	+++		acc		acc				+	+	+	
MP2-10	Mudstone	+++	acc	+	acc					+	acc	+	
MP2-7	Mudstone	+		acc						+++	acc	+	acc
MP2-4	Mudstone	+++		acc				acc		+	acc	+	
MP2-3	Mudstone	++			acc				acc	++	acc	acc	
K7													
KT2-1	Mudstone	+++	acc							+	+	+	
KT2-2	Mudstone	+++	acc							++	+	+	
KT2-3	Mudstone	+++		+						+++	+	acc	
KT2-5	Mudstone	++++	acc	acc						++	acc	+	
KT2-7	Mudstone	++++	acc	acc						+	acc	+	
KT2-8	Mudstone	++++								acc	+	acc	acc
KT2-10	Mudstone	+++								acc	acc	acc	+
KT2-11	Mudstone	+++								+	acc	+	acc
Middle													
K6													
AKB-11	Mudstone	++++								acc	+	+	
AKB-10	Mudstone	++++								acc	+	+	
AKB-9	Mudstone	++	acc							acc	+		++
AKB-7	Mudstone	+++	acc		+					acc	+	acc	+
AKB-5	Mudstone	++	acc		acc					acc	+		++
AKB-4	Mudstone	++		acc	acc			+		+	+		++
K5													
C-2	Mudstone	+++	acc		acc	acc				+	+	acc	
C-3	Mudstone	+++								acc	+	acc	+
C-4	Mudstone	++			acc		acc			+	+		++
C-5	Mudstone	++				acc				+	+	+	
K4													
YH-2	Mudstone	++	acc		acc			acc		+	+	acc	++
YH-5	Mudstone	++			acc					acc	+		+
YH-7	Mudstone	++	acc	acc	+					acc	+		+
YH-10	Mudstone	++	acc		acc		acc			+	+		+
YH-11	Mudstone	++			acc		+		acc	+	+	acc	acc
YH-13	Mudstone	+++		acc	acc		+			acc	+	acc	++
K3													
AT-5	Mudstone	+++		acc						acc	+		+
AT-8	Mudstone	++								+	+		acc
South													
K2													
A22N-11	Mudstone	++++								acc	+		
A22N-4	Mudstone	++++									+		
K1													
HB-2	Mudstone	+++								acc	+		
HB-3	Matrix of Yeşilhisar conglomerate	++++					acc		acc	acc	+		acc
HB-5	Mudstone	++++	acc	acc						acc	+		acc

smc: smectite, ilt/mc: illite/mica, kln: kaolinite, chl: chlorite, srp: serpentine, am: amphibole, px: pyroxene, ol: olivine; fds: feldspar, qz: quartz, op: opal-A, cal: calcite. acc: accessory, +: relative abundance of mineral.

https://doi.org/10.1346/CCMN.2014.0620403 Published online by Cambridge University Press

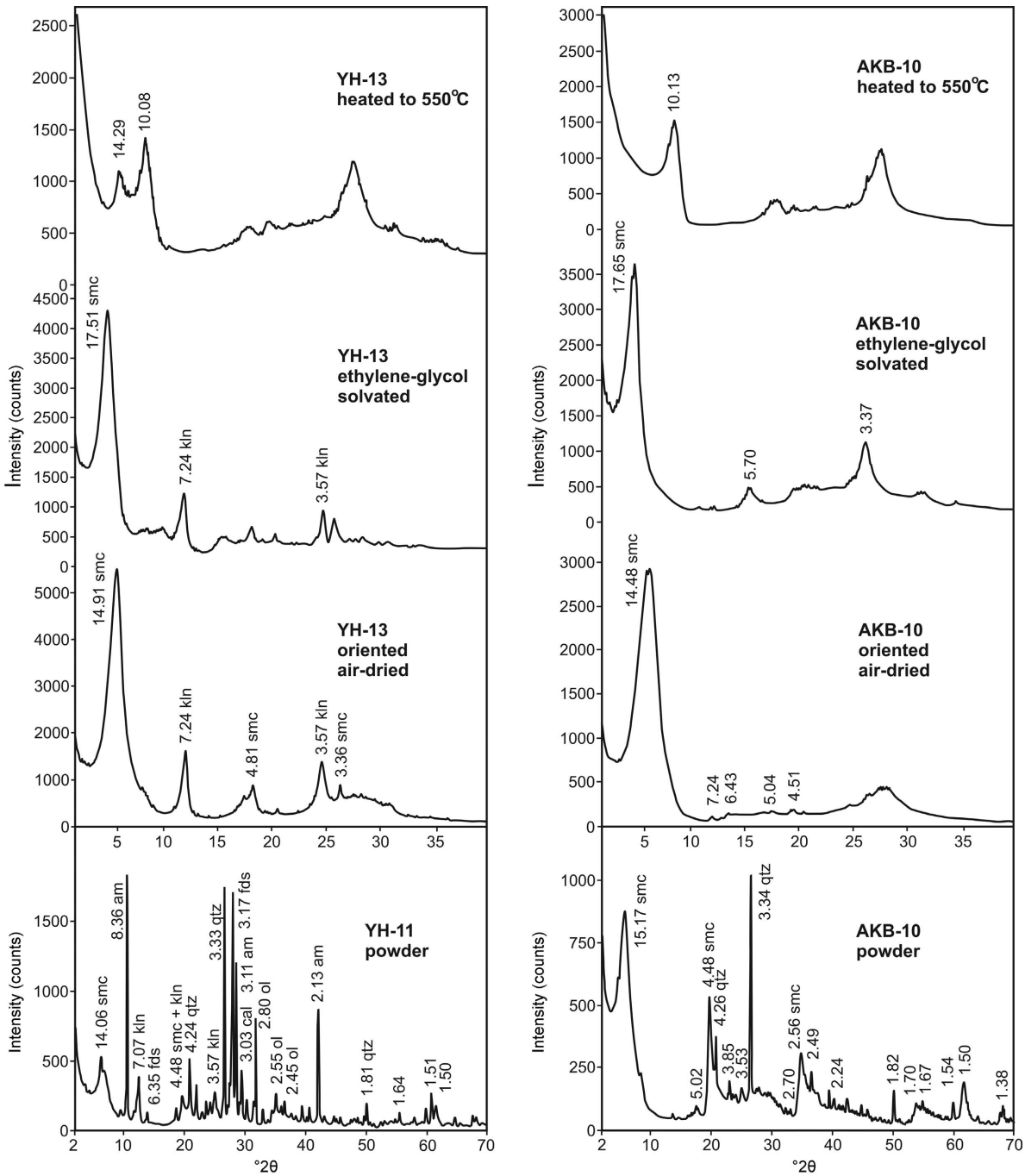

Figure 5. XRD patterns of smectite-rich mudstone samples (YH-11, YH-13, AKB-10). smc: smectite, kln: kaolinite, fds: feldspar, qz: quartz, am: amphibole, ol: olivine, cal: calcite.

at 10.0 and 5.0 Å, which are not affected by the ethylene-glycol treatment but undergo a slight shift toward a higher angle when heated to 550ºC because of dehydroxylation. Kaolinite has peaks at 7.24 and 3.57 Å and serpentine has peaks at 7.63 Å. Sharp peaks appear in amphibole at 8.36 and 3.11 Å, in pyroxene at 2.90 Å, in olivine at 2.80 Å, in quartz at 3.34 and 4.26 Å, in feldspar at 3.18 Å, and in calcite at 3.03 Å. An increase in the XRD background intensity in some of the samples may indicate the presence of opal-A (Iijima and Tada, 1981).

Amphibole is associated with accessory chlorite, serpentine, and olivine and is found mainly in weathered ophiolitic units, related to weathered units of the Araplı area in the southern region of the studied area. Illite and feldspar increase northward near the Akköy area.

https://doi.org/10.1346/CCMN.2014.0620403 Published online by Cambridge University Press

SEM-EDX AND TEM DETERMINATIONS

Scanning electron microscope images indicate that flaky smectite predominates in the mudstone and matrix of the Yeşilhisar conglomerate samples (Figure 6). Flaky smectite crystals (up to 2−7 μm in diameter) appear in the samples with irregular outlines and are locally edged with fibrous illite (Figure 6a−h). Amphiboles with rod-like forms (~10 μm long) and pyroxene relics are associated with smectite in the mudstones from the southern part of the study area (Figure 6c,d). Smectite in the northern mudstones occur as authigenic flakes and include relict crystals, such as feldspar and devitrified volcanic glass (Figure 6e,f). In addition, irregular flaky smectite in the central mudstone encloses authigenic euhedral micritic calcite crystals (1−7 μm in diameter) as regular pore fillings (Figure 6g,h).

Energy dispersive analyses of the smectite flakes have large peaks for Si, Al, Fe, and Ca and low Al and Mg (Figure 7a). Energy dispersive analyses of rod and rod-bundle amphibole crystals yielded Si, Ca, and Fe and low Al, whereas the pyroxene precursor exhibits high Ca, Fe, and Si and low Mg resembling augite-type pyroxenes (Figure 7b,c). Relics of feldspars exhibit high peaks for Si, smaller peaks for Al, and very faint peaks for K and Ca (Figure 7d). The altered volcanic rocks consist mainly of Si with very small peaks for Al, Mg, K, Ca, and Na (Figure 7e). Rhombic calcite crystals exhibit strong peaks for Ca (Figure 7f).

Transmission electron microscope analyses indicate that the smectite particles occur as wavy fan- and lens-like plate packets arranged in a well oriented order (Figure 8a−f). In addition, there are discontinuous, bent and non-oriented packs of smectite particles (Figure 8b−f). Smectite plates edge rod-like crystals of amphiboles in the mudstones (Figure 8d−f). The sharp edges of the individual fibers suggest moderate to high crystallinity. The smectite plates have a diameter of 300−600 nm.

Geochemistry

Chemical analyses of representative samples of ophiolite and the associated Yeşilhisar conglomerate matrix, mudstones, and ignimbrites in the Cappodocia region are given in Table 2 (please see an extended version of this table which has been deposited with the Editor in Chief and is available from http://www.clays.org/JOURNAL/JournalDeposits.html). The variations in the major and trace-element profiles appear to be related to ophiolitic and volcanic provenances (Table 2, plus extended version, deposited). Therefore, SiO_2, K_2O, TiO_2, Σ*REE*, and Zr values increase and Fe_2O_3 and MgO values decrease northward in the mudstones of the Mustafapaşa member. The loss on ignition is an important indicator of weathering and is proportional to the amount of calcite and clay minerals. Large amounts of Cr, Ni, and Co are found in the ophiolitic rocks with average values of 1850, 1917, and 98.5 ppm, respectively. The Cr, Ni, and Co contents decrease from the south to the middle to the north with average values in the mudstones of the Mustafapaşa member of 548, 475, and 40 ppm; 402, 226, and 26 ppm; and 136, 46, and 15 ppm, respectively. In addition, the Ba, Rb, and Sr contents of the sediments of the Mustafapaşa member display local increases northward.

SiO_2 has a positive correlation with K_2O, and Σ*REE* correlates positively with Zr in the mudstone samples (Figure 9a,b). A plot of Zr/Ni *vs.* Zr/Co shows a northward increase in Zr content relative to Ni and Co (Figure 10).

The whole-rock *REE* contents of samples from the study area were normalized to the North American Shale Composite (NASC) values (Gromet *et al.*, 1984) (Figure 11). Light *REE*s (*LREE*s), such as La, Ce, and Nd, are enriched relative to the increase in concentrations of medium *REE*s (*MREE*s) and heavy *REE*s (*HREE*s) based on the increase in La_N/Yb_N ratios from 0.41 to 5.96 in mudstones from south to north in the study area (Table 1, Figure 11a−c). However, *LREE*s were leached relative to the *MREE*s and *HREE*s in mudstone samples close to the ophiolitic units and related Yeşilhisar conglomerates in the southern region (Table 1, Figure 11a,d). Nb/Ti increases parallel to the increase in La/Yb northward (Figure 12). The *LREE*/*HREE* ratio is enriched in ignimbrite samples (Figure 11e).

The averages [$(Eu/Eu^*)_{NASC}$= 0.98−1.67 and $(Ce/Ce^*)_{NASC}$ = 0.75−1.06] show positive Eu and negative Ce anomaly values, respectively (Table 2, deposited). The $(Yb/Yb^*)_{NASC}$ ratios range from 0.80 to 1.17 and are positive, revealing a relatively immobile character.

The structural formulae of smectite were calculated from chemical analyses of the clay fractions of samples A22N-11, AKB-11, and KT2-8 (Table 3). The average structural formula was estimated to be $(Si_{7.59}Al_{0.41})(Al_{2.34}Fe_{0.93}Mg_{0.76}Ti_{0.06}Mn_{0.013})(Ca_{0.29}Na_{0.03}K_{0.20})O_{20}(OH)_4$. The tetrahedral site is filled by Si, which is substituted by a small amount of Al. Al is the predominant cation in the octahedral site and is accompanied by Fe^{3+}, Mg, and traces of Ti and Mn. Ca, Na, and K were deemed exchangeable interlayer cations. The average tetrahedral charge/octahedral charge ratio (xt/xo) is 1.00. These values indicate that the smectite is montmorillonite, similar to that reported by Güven (1988) and Inoue *et al.* (2004).

DISCUSSION

The basement rocks in the study area consist of Paleozoic and Mesozoic gneiss, marble, and ophiolitic rocks. Long-term weathering of ophiolite and ignimbrite units from the Early Eocene to the Late Miocene produced an enormous amount of argillaceous material that was later transported and deposited in the depressional basin

https://doi.org/10.1346/CCMN.2014.0620403 Published online by Cambridge University Press

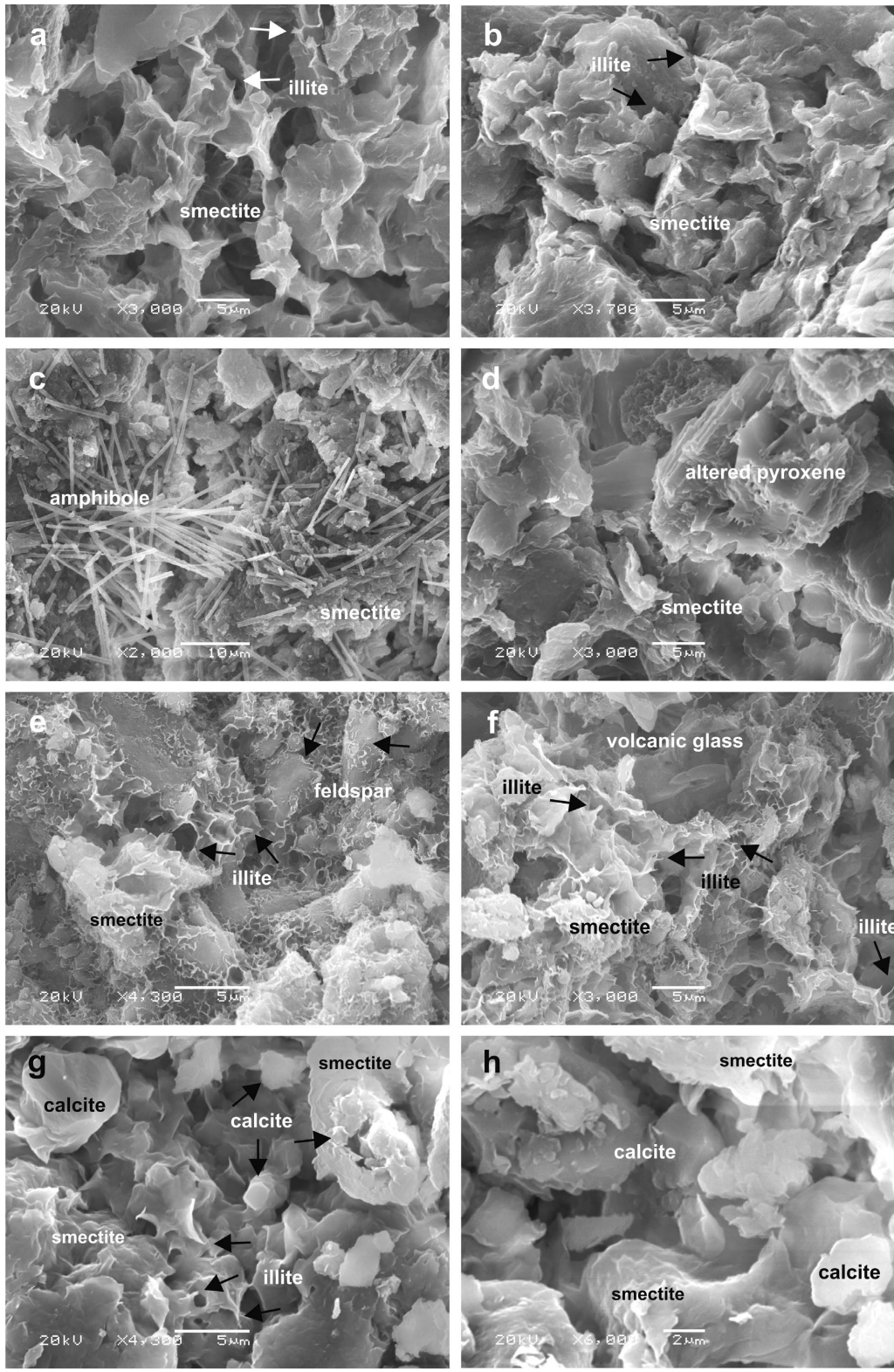

Figure 6. SEM images: (a,b) irregular cornflake-shaped smectite in southern mudstones (YH11, A22N-11); (c) smectite flakes with rod-like amphibole crystals (YH-13); (d) altered pyroxene edging smectite flakes (KT2-8); (e,f) authigenic growth of smectite on and between altered feldspar crystals and devitrified volcanic glass (AKB-13); (g,h) authigenic growth of calcite crystals in pores of irregular smectite and smectite-edged illite (AKB-8).

https://doi.org/10.1346/CCMN.2014.0620403 Published online by Cambridge University Press

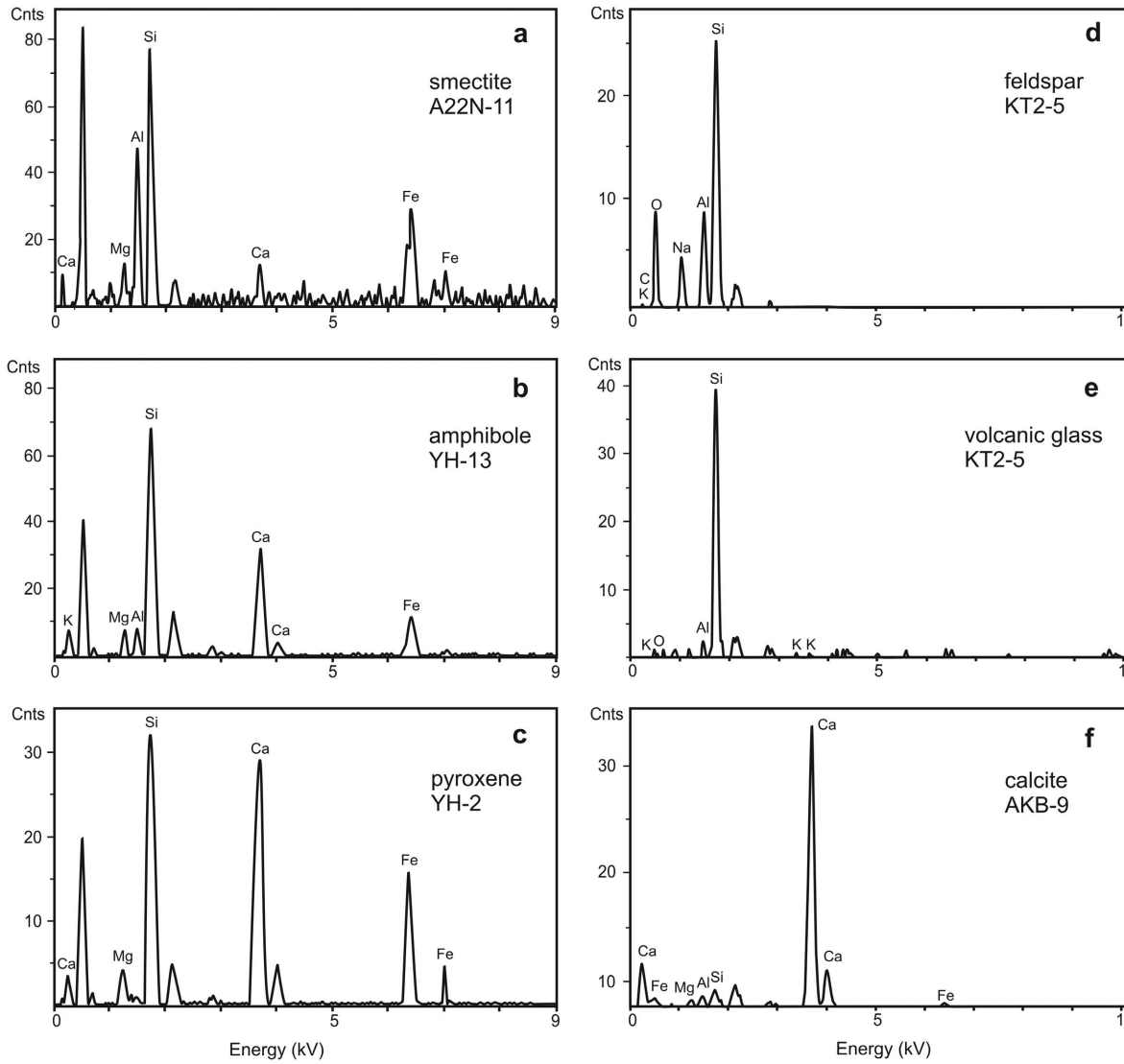

Figure 7. EDX analyses of smectite and precursors in mudstone samples.

as fluvial and lacustrine deposits. Evidence of weathering is seen in smectite flakes in the mudstones, which are associated with relict pyroxenes, rod-like amphiboles, feldspars, and volcanic glass (Figure 6). The suggestion of a detrital origin for the smectitic mudstone is based mainly on its repetition in stratigraphic sections and its matrix form in conglomerates, associated discrete minerals derived from ophiolitic and volcanogenic rocks (Hong *et al*., 2007, 2012) and micromorphologies of smectite flakes with irregular boundaries.

Changes in the concentrations of Fe_2O_3+MgO, Al_2O_3, and SiO_2 in the mudstones of the Mustafapaşa member are caused by vertical and lateral variations in lithologies. The presence of Fe_2O_3+MgO in the sediments may indicate detrital pyroxene, amphibole, and Fe (oxyhydr)oxide phases from ultramafic units exposed in the south and SiO_2 and Al_2O_3 from volcanogenic materials, such as feldspars and opal-A in the northern region. Therefore, smectitic mudstones from the southern region contain more Fe±Mg and less Si±Al and Ca+K+Na than either the middle or northern parts (Table 3). After the deposition of smectitic mudstones, the local concentration of Ca and K (along with Al) in the pore water resulted in *in situ* formation of calcite cement filling the micropores.

The edging of irregular smectite flakes by trace illite developed as a result of a dissolution and precipitation mechanism under alkaline micro-environmental conditions during early diagenesis (Braide and Huff, 1986; Erhenberg, 1991; Meunier and Velde, 2004; Ziegler, 2006). The presence of trace kaolinite in the northern part was caused by the relative increase of altered feldspars, amphiboles, and volcanic glass in the volcanic input throughout the sequence.

https://doi.org/10.1346/CCMN.2014.0620403 Published online by Cambridge University Press

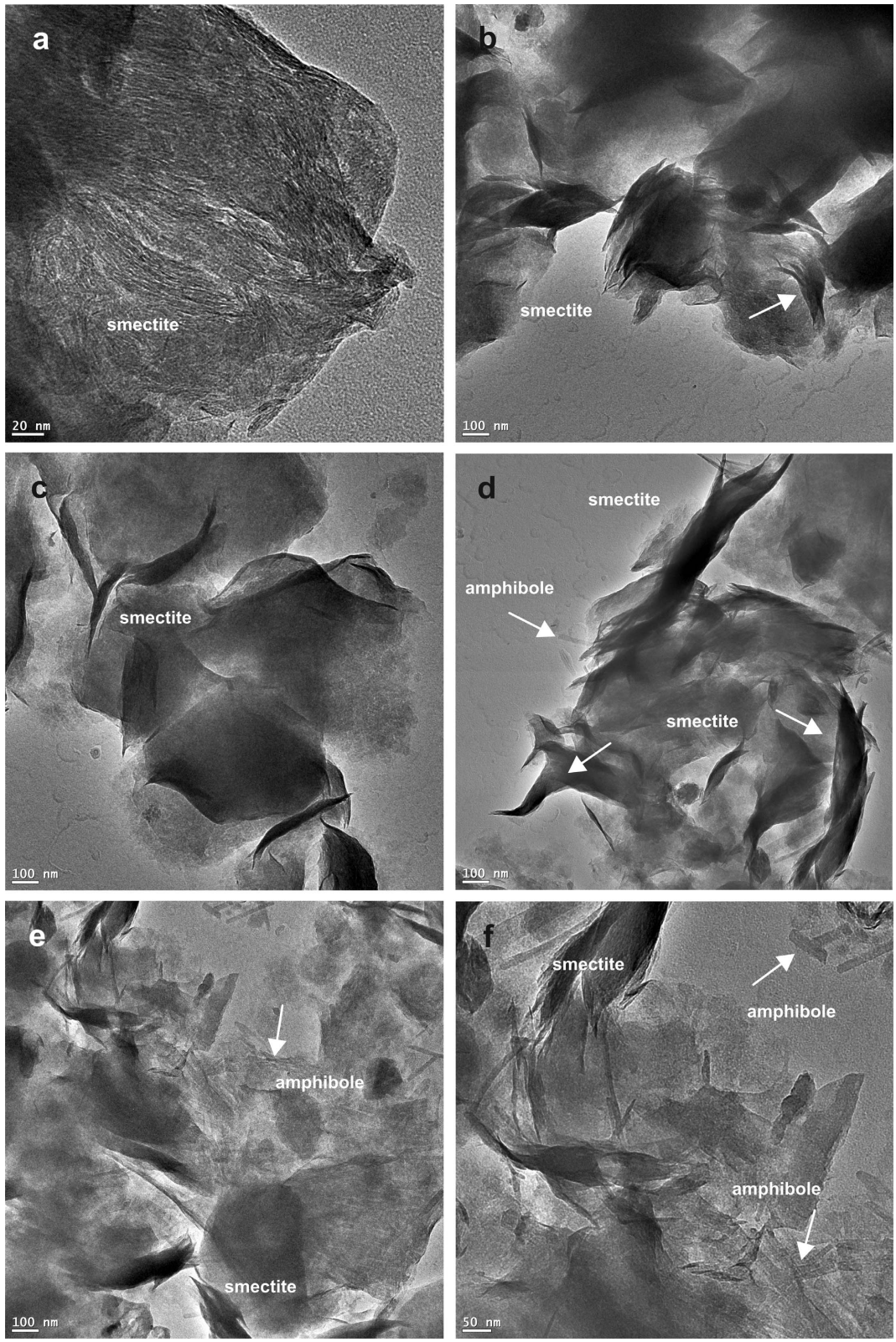

Figure 8. TEM images showing: (a) smectite plates, plate bundles (A22N-11); (b–d) wavy fan- and lens-like smectite plate packets (A22N-11, AKB-11); (d–f) smectite plates edging rod-like amphiboles (AKB-11), and (c–d) smectite plates edging fibrous materials resembling illite (A22N-11, AKB-11).

https://doi.org/10.1346/CCMN.2014.0620403 Published online by Cambridge University Press

Table 2. Major oxides (wt.%), trace elements (ppm), and *REE* contents (ppm) of ophiolite, the Yeşilhisar conglomerate matrix, mudstones, and ignimbrites in the study area.

Major oxides (wt.%)	Ophiolite	Yeşilhisar matrix	Mudstone			Ignimbrite
			South	Middle	North	
	Avg. (n = 3)	(n = 1)	Avg. (n = 4)	Avg. (n = 11)	Avg. (n = 8)	Avg. (n = 2)
SiO_2	39.04	58.57	50.35	44.70	57.87	70.2
Al_2O_3	1.1	19.04	16.95	11.70	15.22	14.29
ΣFe_2O_3	8.05	4.58	9.12	6.23	6.11	1.73
MgO	36.51	2.15	4.38	4.24	1.57	0.39
CaO	0.16	1.26	2.71	11.68	3.1	1.76
Na_2O	0.003	1.83	2.09	1.24	1.57	2.33
K_2O	–	0.41	0.56	0.92	1.74	3.64
TiO_2	0.006	0.68	0.50	0.58	0.56	0.26
P_2O_5	–	0.02	0.04	0.08	0.11	0.03
MnO	0.07	0.02	0.07	0.09	0.06	0.05
LOI	13.8	11.2	13.2	18.3	12.0	5.2
Total	99.37	99.88	99.86	99.84	99.83	99.90
Trace elements (ppm)						
Ba	5	61	50.25	144.3	609	760.5
Be	0.33	2	1	1.7	1.5	2
Co	98.53	34.8	40.05	26	14.8	3.5
Cr	1850	590	547.5	401.8	136.25	80
Cs	–	0.9	3.43	6.3	3.4	4.9
Ga	0.73	17.3	13.48	10.9	14.2	13.5
Hf	–	2.4	1.4	2.3	3.8	4.2
Nb	–	2.6	3.1	6	8.8	4.2
Ni	1917	567	474.8	226.3	46	34
Rb	0.16	10.4	29.3	42.3	76.4	122.8
Sc	8	44	27.5	18.3	12.1	3.5
Sn	0.33	–	–	0.4	0.6	–
Sr	5	72.2	100.4	216.3	222.3	217.4
Ta	–	0.2	0.26	0.4	0.6	0.9
Th	–	1.5	1.9	5.4	12.7	21.9
U	0.3	0.4	1.9	1.6	2.6	6.45
V	37.3	255	127.5	109	72	5.5
W	0.43	–	1.05	1.6	2.2	2.7
Zr	0.4	77.1	51.2	85.2	145.7	148
Y	0.2	38.9	10.25	15.4	19.5	15.6
La	0.13	9.8	4.7	15.1	24.6	36.9
Ce	0.13	26.1	10.3	26.7	44.4	60.4
Pr	–	3.87	1.17	3.29	4.87	5.93
Nd	–	19.5	5.33	12.7	17.8	20
Sm	–	5.82	1.29	2.63	3.20	3.05
Eu	–	1.96	0.42	0.73	0.85	0.64
Gd	–	7.26	1.58	2.65	3.10	2.6
Tb	–	1.23	0.26	0.42	0.50	0.39
Dy	–	7.30	1.77	2.73	3.20	2.44
Ho	–	1.52	0.37	0.55	0.68	0.52
Er	–	4.62	1.09	1.56	1.93	1.59
Tm	–	0.60	0.16	0.22	0.30	0.26
Yb	0.23	3.77	1.16	1.55	2.16	1.89
Lu	–	0.56	0.18	0.23	0.34	0.29
TOT/C	0.1	0.03	0.24	2.42	0.26	0.15
TOT/S	–	0.03	0.25	0.04	0.004	–
Mo	0.07	0.2	0.9	0.3	0.2	1.5
Cu	12.73	30.3	56.46	24.8	13.0	3.3
Pb	0.33	3.2	3.8	8.24	5.8	1.7
Zn	18.3	52	52.5	38.6	19.5	7.5
Ni	2017.8	377.3	315.7	204.0	20.7	32.7
As	3.1	4.7	8.1	6.9	14.8	–
Cd	–	–	–	0.05	–	–
Sb	–	–	0.05	0.12	0.03	–

https://doi.org/10.1346/CCMN.2014.0620403 Published online by Cambridge University Press

Table 2 (*contd*.)

Major oxides (wt. %)	Ophiolite	Yeşilhisar matrix	Mudstone			Ignimbrite
			South	Middle	North	
	Avg. (n = 3)	(n = 1)	Avg. (n = 4)	Avg. (n = 11)	Avg. (n = 8)	Avg. (n = 2)
Bi	–	–	0.05	0.07	0.11	0.05
Ag	–	–	–	–	–	–
Au (ppb)	2.6	–	0.9	1.2	1.5	1.2
Hg	0.003	–	0.02	0.02	0.001	–
Tl	–	–	–	0.08	0.1	–
Se	–	0.6	–	–	0.01	–
Σ*REE*	0.69	132.8	40.03	86.46	127.4	152.5
Σ*LREE*	0.26	59.27	21.50	59.40	91.70	123.2
Σ*MREE*	0.2	25.09	5.69	9.71	11.5	10.4
Σ*HREE*	0.1	9.55	2.59	5.45	4.73	4.82
Eu/Eu*	1.75	1.30	1.26	1.26	1.20	1.04
Ce/Ce*	0.63	0.89	0.92	0.83	0.87	0.97
Yb/Yb*	0.89	1.02	1.09	1.09	1.06	1.32
La_N/Yb_N	0.3	0.25	0.41	0.94	5.96	14.42

n: number of samples.
Σ*REE* = the sum of (La–Lu)+Y; Σ*LREE* = the sum of La–Nd; Σ*MREE* = the sum of (Sm–Ho); Σ*HREE* = the sum of (Er–Lu); $Ce/Ce^* = 2Ce_N/(La_N+Pr_N)$, $Eu/Eu^* = 2Eu_N/(Sm_N+Gd_N)$, $Yb/Yb^* = 2Yb_N/(Tm_N+Lu_N)$, where N refers to a NASC-normalized value (Gromet *et al.*, 1984).

The *LREE*s/*HREE*s in a NASC-normalized pattern and the $(La/Yb)_N$ ratios are correlated positively with the concentration of smectite in the mudstone deposits and increase from south to north, indicating an increasing contribution of volcanic materials in that direction. Therefore, the fractionation of amphibole and feldspar resulted in the adsorption of *LREEs* onto the smectite and Fe (oxyhydr)oxide phases, similar to that reported by Christidis (1998) and Jeans *et al.* (2000). However, the depletion of *LREE*s relative to *MREE*s and *HREE*s in mudstones from the southern region suggests that they benefited from the alteration of amphibole and pyroxene that originated from the ophiolitic basement rock (Cullers and Graf, 1983; Nyakairu and Koeberl, 2001). A positive Eu anomaly value suggests that the accumulation and alteration of plagioclase originated from the input of interlayered volcanic units (Nance and Taylor, 1977).

The parallel northward increase in the Nb/Ti abundance ratio relative to the La/Yb ratio suggests that Nb and La are concentrated with increasing smectite-dominated mudstone deposits derived mainly from ophiolite and related Yeşilhisar conglomerates and volcanic source rocks. This was confirmed by a northward parallel increase in the Zr/Ni ratio relative to the Zr/Co ratio and a positive correlation of Zr with Σ*REE* in the mudstone samples. This suggests that Σ*REE* have a similar geochemical behavior associated with the molecular structure of smectite, which increases northward with Zr. This interpretation is also supported by an increase in Ba, Rb, and Sr in the mudstones of the Mustafapaşa member to the north, close to the Kavak and Sarımadentepe ignimbrites, and by the increase in Ni, Co, and Cr in the mudstones in the south, near the ophiolitic basement units. Intermediate values of these data are present in the mudstones in the middle area.

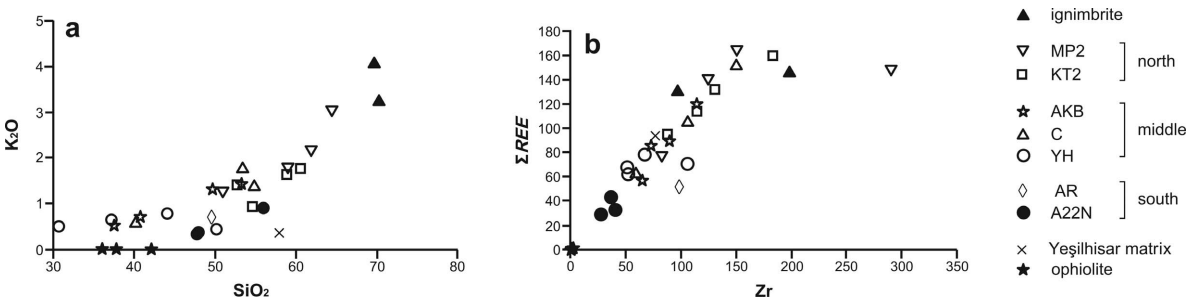

Figure 9. Elemental variation diagrams for major oxides (wt.%) and trace elements of the Cappadocia region samples: (a) SiO_2 *vs*. K_2O; (b) Zr *vs*. Σ*REE*.

https://doi.org/10.1346/CCMN.2014.0620403 Published online by Cambridge University Press

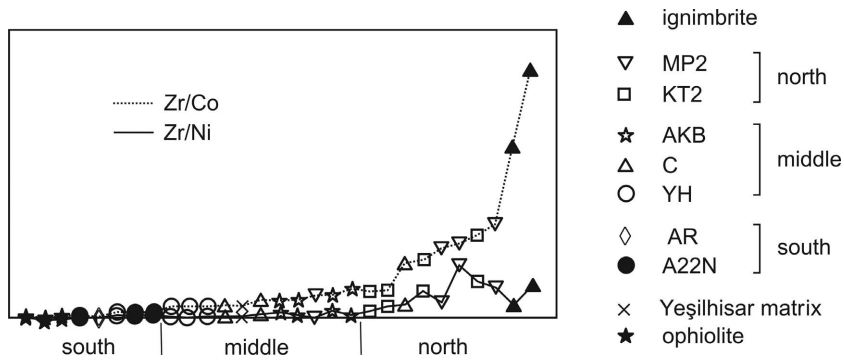

Figure 10. Plots of Zr/Ni *vs*. Zr/Co for the smectite-dominated mudstone samples from the south, middle, and north of the study area.

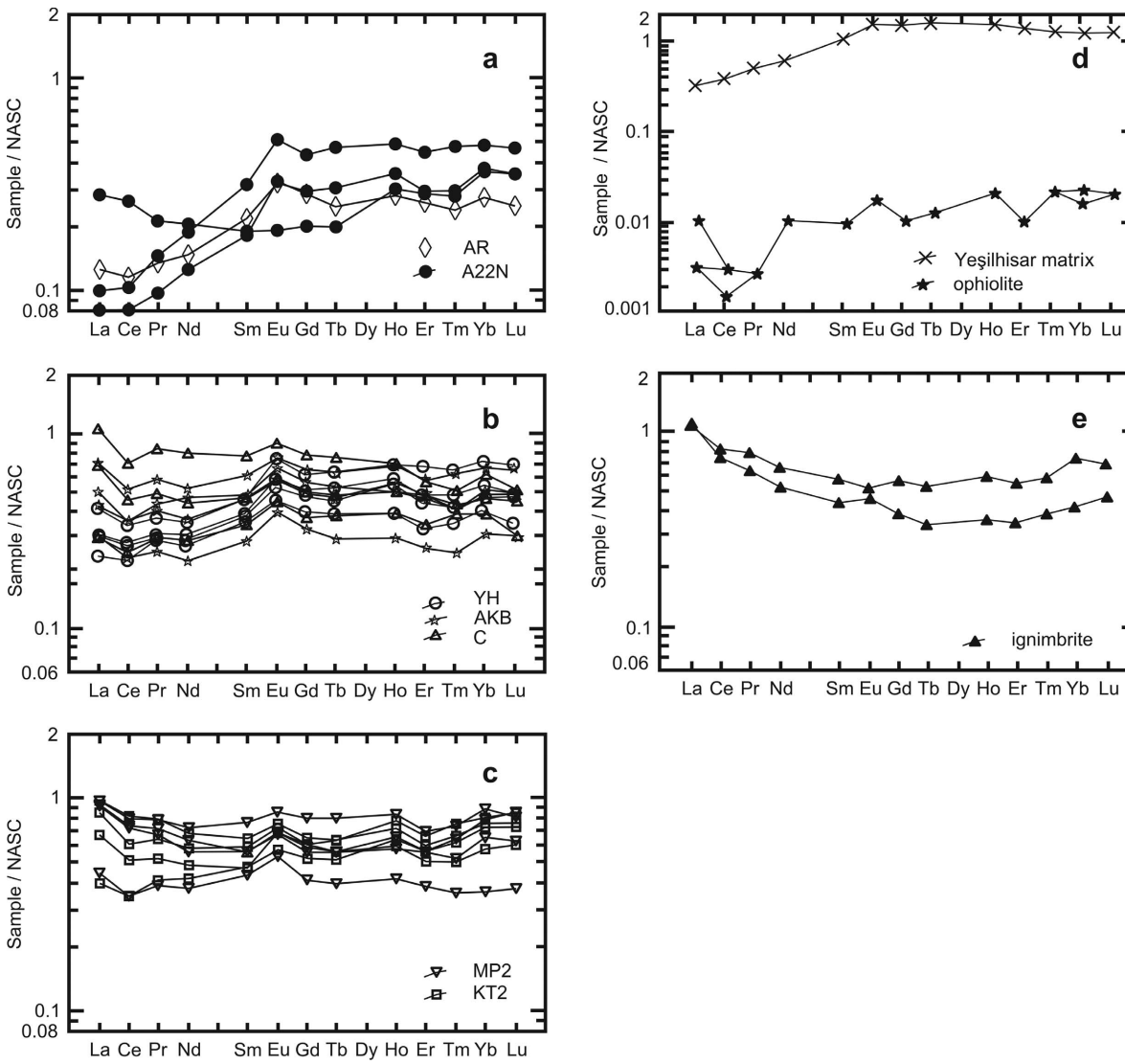

Figure 11. NASC-normalized *REE* patterns (Gromet *et al.*, 1984) from the smectite-dominated mudstone samples from: (a) the south; (b) the middle; (c) the north, and (d,e) north of the study area.

https://doi.org/10.1346/CCMN.2014.0620403 Published online by Cambridge University Press

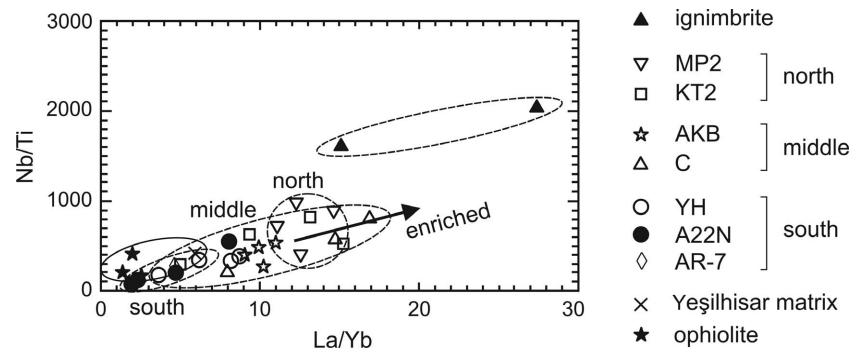

Figure 12. Plots of La/Nb *vs.* Nb/Ti for the smectite-dominated mudstone samples from the south, middle, and north of the study area.

Table 3. Chemical compositions (wt.%) and structural formulae for pure smectite samples.

Major oxides (wt.%)	A22N-11 South	AKB-11 Middle	KT2-8 North	Average
SiO_2	49.20	50.93	51.0	50.38
Al_2O_3	15.30	15.80	15.30	15.47
ΣFe_2O_3	11.08	6.19	7.31	8.20
MgO	2.84	4.09	3.17	3.37
CaO	1.62	1.58	2.20	1.80
Na_2O	0.03	0.07	0.18	0.09
K_2O	0.84	1.42	0.94	1.07
MnO	0.06	0.10	0.07	0.08
TiO_2	0.42	0.53	0.59	0.51
LOI	18.2	19.0	19.0	18.73
Total	99.59	99.71	99.76	99.69
SiO_2/Al_2O_3	3.22	3.22	3.33	3.26
Tetrahedral				
Si	7.45	7.65	7.68	7.59
Al	0.55	0.35	0.32	0.41
Σ	8.00	8.00	8.00	8.00
Octahedral				
Al	2.18	2.45	2.39	2.34
Fe	1.26	0.70	0.83	0.93
Mg	0.65	0.92	0.72	0.76
Ti	0.05	0.06	0.07	0.06
Mn	0.009	0.02	0.01	0.013
Σ	4.15	4.15	4.02	4.11
Interlayer				
Ca	0.262	0.254	0.355	0.29
Na	0.009	0.01	0.052	0.03
K	0.162	0.272	0.180	0.20
Σ	0.433	0.536	0.587	0.52
Tetrahedral charge	0.550	0.350	0.320	0.41
Octahedral charge	0.170	0.450	0.610	0.41
Total charge	0.720	0.800	0.930	0.82
Interlayer charge	0.690	0.800	0.930	0.81
xt/xo	3.24	0.78	0.52	1.00

xt/xo = tetrahedral charge/octahedral charge ratio.

https://doi.org/10.1346/CCMN.2014.0620403 Published online by Cambridge University Press

However, a slight to moderate negative Ce anomaly in mudstones and ophiolites suggests the substitution of Ce by Fe in iron-oxide/hydroxide phases under oxidizing and reducing sedimentation environments (Fulignati *et al.*, 1999; Karakaya, 2009; Zhou *et al.*, 2013). This suggestion was supported by the alternation of green, yellow, and dark red mudstones, reflecting the fluctuation of reducing and oxidizing conditions in the depositional environment (Eren and Kadir, 2013).

CONCLUSIONS

The development of flaky smectite and smectite ± illite with relict pyroxenes, amphiboles, feldspars, and volcanic glass suggests that the weathering of ophiolitic units in the south and volcanic units in the north contributed to the accumulation of detrital smectite-dominated fluvial and lacustrine mudstone deposits of the Mustafapaşa member in a tectonic depressional basin. Serpentinized and Fe (oxyhydr)oxide-bearing pyroxenes and amphiboles, and the alteration of feldspars, originated from the weathering of ophiolitic units, related Yeşilhisar conglomerates, and ignimbrites. Increases in the *LREE*s/*HREE*s, $(La/Yb)_N$, Zr/Ni, and Zr/Co ratios and Ba, Rb, and Sr in the mudstones in the northern Mustafapaşa member with a positive Eu anomaly suggest that the decomposition of detrital materials from ophiolitic and volcanogenic material were the main sources of Fe±Mg, Al, and Si for the smectite in mudstones in the study area. Therefore, the change in the chemical composition of smectite fractions in the depressional basin is related mainly to the proximity to the source area.

ACKNOWLEDGMENTS

The present study was supported financially by the Scientific Research Projects Fund of Eskişehir Osmangazi University in the framework of Project 201015030 and constitutes part of the PhD thesis of the first author. The authors are much indebted to anonymous reviewers for their extremely careful and constructive reviews which improved the quality of the paper significantly. The authors are also grateful to Associate Editor, Warren D. Huff, and Editor in Chief, Michael A. Velbel, for their insightful editorial comments and suggestions.

REFERENCES

Batum, I. (1975) Petrographische und geochemische Untersuchungen in den Vulkangebieten Göllü Dağ und Acıgöl (Zentralanatolien/Türkei). PhD thesis, Freiburg University, Germany, 101 pp.

Batum, I. (1978) Geology and petrography of the Göllüdağ and Acıgöl volcanics in the southwestern Nevşehir. *Bulletin of Earth Sciences Application and Research Centre of Hacettepe University*, **4**, 50–69. (In Turkish with English abstract.)

Besang, C., Eckhardt, F.J., Harre W., Kreuzer, H., and Müller, P. (1977) Radiometrische Altersbestimmungen an Neogenen eruptivgesteinen der Turkei. *Geologisches Jahrbuch*, **B25**, 3–36.

Braide, S.P. and Huff, W.D. (1986) Clay mineral variation in Tertiary sediments from the eastern Flank of the Niger Delta. *Clay Minerals*, **21**, 211–224.

Brindley, G.W. (1980) Quantitative X-ray analysis of clays. Pp. 411–438 in: *Crystal Structures of Clay Minerals and their X-ray Identification* (G.W. Brindley and G. Brown, editors). Monograph **5**, Mineralogical Society, London.

Casciello, E., Cosgrove, J.W., Cesarano, M., Romero, E., Queralt, I., and Vergés, J. (2011) Illite-smectite patterns in sheared Pleistocene mudstones of the southern Apennines and their implications regarding the process of illitization: a multiple analysis. *Journal of Structural Geology*, **33**, 1699–1711.

Chermak, J.A. and Schreiber, M.E. (2014) Mineralogy and trace element geochemistry of gas shales in the United States: Environmental implications. *International Journal of Coal Geology*, **126**, 32–44.

Christidis, G.E. (1998) Comparative study of the mobility of major and trace elements during alteration of an andesite and a rhyolite to bentonite, in the islands of Milos and Kimolos, Aegean, Greece. *Clays and Clay Minerals*, **46**, 379–399.

Cullers, R.L. and Graf, J. (1983) Rare earth elements in igneous rocks of the continental crust: intermediate and silicic rocks, ore petrogenesis. Pp. 275–312 in: *Rare-Earth Geochemistry* (P. Henderson, editor). Elsevier, Amsterdam.

Delvigne, J.E. (1998) *Micromorphology of Mineral Alteration and Weathering*. *The Canadian Mineralogist*, Special Publication, 494 pp.

Dilek, Y. and Furnes, H. (2014) Ophiolites and their origins. *Elements*, **10**, 93–100.

Dilek, Y. and Whitney, D.L. (1997) Counterclockwise *P-T*-t trajectory from the metamorphic sole of a Neo-Tethyan ophiolite (Turkey). *Tectonophysics*, **280**, 295–310.

Druitt, T.H., Brenchley, P.J., Gökten, Y.E., and Francaviglia, V. (1995) Late Quaternary rhyolitic eruptions from the Acıgöl complex, Central Turkey. *Journal of Geological Society*, London, **152**, 655–667.

Ercan, T., Köse, C., Akbaşli, A., and Yildirim, T. (1987) Orta Anadolu'da Nevşehir-Niğde-Konya dolayındaki volkanik kökenli gaz çıkışları. *Cumhuriyet Üniversitesi Mühendislik Fakültesi Dergisi – Seri A, Yerbilimleri*, **4**, 57–63.

Ercan, T., Yeğingil, Z., and Biggazi, G. (1989) Obsidiyen tanımı ve özellikleri, Anadolu'daki dağılımı ve Orta Anadolu obsidiyenlerinin jeokimyasal nitelikleri. *Jeomorfoloji Dergisi*, **17**, 71–83.

Eren, M. and Kadir, S. (2013) Colour origin of red sandstone beds within the Hüdai Formation (Early Cambrian), Aydıncık (Mersin), southern Turkey". *Turkish Journal of Earth Sciences*, **22**, 563–573.

Erhenberg, S.N. (1991) Kaolinized, potassium-leached zones at the contacts of the Garn Formation, Haltenbanken, mid-Norwegian continental shelf. *Marine and Petroleum Geology*, **8**, 250–269.

Fulignati, P., Gioncada, A., and Sbrana, A. (1999) Rare-earth element (REE) behaviour in the alteration facies of the active magmatic-hydrothermal system of Vulcano (Aeolian Islands, Italy). *Journal of Volcanology and Geothermal Research*, **88**, 325–342.

Gevrek, A.İ. (1997) Aksaray doğusu, Ihlara-Derinkuyu yöresindeki volkaniklastiklerin sedimentolojisi. Doktora Tezi, Ankara Üniversitesi Fen Bilimleri Enstitüsü, 178 pp. (in Turkish, unpublished).

Göncüoğlu, C. and Toprak, V. (1992) Neogene and Quaternary volcanism of Central Anatolia: a volcano-structural evaluation. *Bulletin de la Section de Volcanologie, Société Géologique de France*, **26**,1–6.

Göz, E., Kadir, S., Gürel, A., and Eren, M. (2014) Geology, mineralogy, geochemistry, and depositional environment of

a Late Miocene/Pliocene fluvio-lacustrine succession, Cappadocian Volcanic Province, central Anatolia, Turkey. *Turkish Journal of Earth Sciences*, **23**, 386–411.

Gromet, L.P., Dymek, R.F., Haskin, L.A., and Korotev, R.I. (1984) The 'North American Shale Composite': its compilation, major and trace element characteristics. *Geochimica et Cosmochimica Acta*, **48**, 2469–2482.

Gürel, A. and Kadir, S. (2006) Geology, mineralogy and origin of clay minerals of the Pliocene fluvial-lacustrine deposits in the Cappadocian Volcanic Province, Central Anatolia, Turkey. *Clays and Clay Minerals*, **54**, 555–570.

Gürel, A. Ciftci, E., and Kerey, I.E. (2007) Sedimentological characteristics of the Cukurbağ formation deposited along the Ecemis Fault Zone (Central Anatolia, Turkey). *Journal of the Geological Society of India*, **70**, 59–72.

Gürel, A. and Kadir, S. (2008) Geology and mineralogy of Late Miocene clayey sediments in the southeastern part of the Central Anatolian Volcanic Province, Turkey. *Clays and Clay Minerals*, **56**, 307–321.

Güven, N. (1988) Smectites. Pp. 497–559 in: *Hydrous Phyllosilicates* (S.W. Bailey, editor). Reviews in Mineralogy, **19**, Mineralogical Society of America, Washington, D.C.

Hong, H., Li, Z., Xue, H., Zhu, Y., Zhang, K., and Xiang, S. (2007) Oligocene clay mineralogy of the Linxia Basin: evidence of paleoclimatic evoution subsequent to the initial stage uplift of the Tibetan Plateau. *Clays and Clay Minerals*, **55**, 491–503.

Hong, H., Wang, C., Zeng, K., Zhang, K., Yin, K., and Li, Z. (2012) Clay mineralogy of the Zhada sediments: Evidence for climatic and tectonic evolution since ~9 Ma in Zhada, southwestern Tibet. *Clays and Clay Minerals*, **60**, 240–253.

Iijima, A. and Tada, R. (1981) Silica diagenesis of Neogene diatomaceous and volcaniclastic sediments in northern Japan. *Sedimentolgy*, **28**, 185–200.

Innocenti, F., Mazzuoli, R., Pasquarè, G., Radicati Di Brozolo, F., and Villari, L. (1975) The Neogene calcalkaline volcanism of Central Anatolia: geochronological data on Kayseri-Niğde area. *Geological Magazine*, **112**, 349–360.

Inoue, A., Meunier, A., and Beaufort, D. (2004) Illite–smectite mixed-layer minerals in felsic volcaniclastic rocks from drill cores, Kakkonda, Japan. *Clays and Clay Minerals*, **52**, 66–84.

Jeans, C.V., Wray, D.S., Merriman, R.J., and Fisher, M.J. (2000) Volcanogenic clays in Jurassic and Cretaceous strata of England and the North Sea Basin. *Clay Minerals*, **35**, 25–55.

Kadir, S., Gürel, A., Senem, H., and Külah, T. (2013) Geology of Late Miocene clayey sediments and distribution of palaeosol clay minerals in the northeastern part of the Cappadocian Volcanic Province (Araplı-Erdemli), central Anatolia, Turkey. *Turkish Journal of Earth Sciences*, **22**, 427–443.

Karakaya, N. (2009) REE and HFS element behaviour in the alteration facies of the Erenler Dağı Volcanics (Konya, Turkey) and kaolinite occurrence. *Journal of Geochemical Exploration*, **101**, 185–208.

Le Pennec, J.L., Bourdier, J.L., Froger, J.L., Temel, A., Camus, G., and Gourgaud, A. (1994) Neogene ignimbrites of the Nevşehir Plateau (Central Anatolia): stratigraphy, distribution and source constraints. *Journal of Volcanology and Geothermal Research*, **63**, 59–87.

Le Pennec, J.L., Temel, A., Froger, J.L., Sen, S., Gourgaud, A., and Bourdier, J.L. (2005) Stratigraphy and age of the Cappadocia ignimbrites, Turkey: reconciling field constraints with paleontologic, radiochronologic, geochemical and paleomagnetic data. *Journal of Volcanology and Geothermal Research*, **141**, 45–64.

Meunier, A. and Velde, B. (2004) *Illite, Origin, Evolution and Metamorphism*. Springer-Verlag, Berlin, Heidelberg, New York, 286 pp.

Moore, D.M. and Reynolds, R.C. (1989) *X-ray Diffraction and the Identification and Analysis of Clay Minerals*. Oxford University Press, New York, 332 pp.

Nahon, D., Paquet, H., and Delvigne, J. (1982) Lateritic weathering of ultramafic rocks and the concentration of nickel in the western Ivory Coast. *Economic Geology*, **77**, 1159–1175.

Nance, W.B. and Taylor, S.R. (1977) Rare earth element patterns and crustal Evolution – II. Archean sedimentary rocks from Kalgoorlie, Australia. *Geochimica et Cosmochimica Acta*, **41**, 225–231.

Nyakairu, G.W.A. and Koeberl, C. (2001) Mineralogical and chemical composition and distribution of rare earth elements in clay-rich sediments from central Uganda. *Geochemical Journal*, **35**, 13–28.

Osborn, S.G., Duffield, L.T., Elliott, W.C., Wampler, J.M., Elmore, R.D., and Engel, M.H. (2014) The timing of diagenesis and thermal maturation of the Cretaceous Marias River Shale, Disturbed Belt, Montana. *Clays and Clay Minerals*, **62**, 112–125.

Pasquarè, G. (1968) Geology of the Cenozoic volcanic area of Central Anatolia. *Atti Della Accademia Nazionale dei Lincei*, *Memorie*, serie VIII, volume **IX**, Roma, 55–204.

Pasquarè, G., Poli, S., Vezzoli, L., and Zanchi, A. (1988) Continental arc volcanism and tectonic setting in Central Anatolia, Turkey. *Tectonophysics*, **146**, 217–230.

Schumacher, R. and Mues-Schumacher, U. (1996) The Kızılkaya ignimbrite-an unusual low-aspect-ratio ignimbrite from Cappadocia, central Turkey. *Journal of Volcanology and Geothermal Research*, **70**, 107–121.

Taylor, K.G. and Macquaker, J.H.S. (2014) Diagenetic alteration in a silt- and clay-rich mudstone succession: an example from the Upper Cretaceous Mancos Shale of Utah, USA. *Clay Minerals*, **49**, 245–259.

Toprak, V. (1998) Vent distribution and its relation to regional tectonics, Cappadocian Volcanics, Turkey. *Journal of Volcanology and Geothermal Research*, **85**, 55–67.

Türkecan, A., Dönmez, M., and Akçay, E.A. (2003) Tertiary volcanics of Kayseri-Niğde-Nevşehir areas. Mineral Research and Exploration Report No. 10575, Ankara (in Turkish, unpublished).

Viereck-Götte, L. and Gürel A. (2003) Klima- und Vegetationswechsel dokumentiert in Obermiozaenen Paläoböden Kappadokiens, Zentralanatolien. *Berichte der Deutschen Mineralogischen Gesellschaft. Beihefte zum, European Journal of Mineralogy*, **15**, pp 211, Stuttgart, Germany.

Viereck-Götte, L., Lepetit, P., Gürel, A., Ganskow, G., Çopuroğlu, İ., and Abratis, M. (2010) Revised volcanostratigraphy of the Upper Miocene to Lower Pliocene Ürgüp Formation, Central Anatolian volcanic province, Turkey. Pp. 85–112 in: *Stratigraphy and Geology of Volcanic Areas* (G. Groppelli and L. Viereck-Götte, editors), *Geological Society of America Special Paper*, 464.

Zhou, L., Zhang, Z., Li, Y., You, F., Wu, C., and Zheng, C. (2013) Geological and geochemical characteristics in the paleo-weathering crust sedimentary type REE deposits, western Guizhou, China. *Journal of Asian Earth Sciences*, **73**, 184–198.

Ziegler, K. (2006) Clay minerals of the Permian Rotliegend Group in the North Sea and adjacent areas. *Clay Minerals*, **41**, 355–393.

(*Received 9 July 2014; revised 17 September 2014; Ms. 895; AE: W.D. Huff*)